Hindawi
Geofluids
Volume 2023, Article ID 4621602, 10 pages
https://doi.org/10.1155/2023/4621602

Research Article

Migration and Release Mechanism of Methane Microseepage Based on Dawanqi Field Work and Physical Simulations

Weiwei Ji,[1] **Guojian Wang**,[2] **Caixin Pu**,[1] **Zhourong Ke**,[1] **Junhong Tang**,[1] **Xufeng Chen**,[3] **Haoqi Wang**,[1] **and Chunhui Wang**[1]

[1]*College of Materials Science and Environmental Engineering, Hangzhou Dianzi University, Hangzhou 310018, China*
[2]*Wuxi Research Institute of Petroleum Geology, Research Institute of Petroleum Exploration and Production, SINOPEC, Wuxi 214126, China*
[3]*College of Sciences, Hangzhou Dianzi University, Hangzhou 310018, China*

Correspondence should be addressed to Junhong Tang; tang_jhjh@163.com

Received 22 August 2022; Revised 28 November 2022; Accepted 29 November 2022; Published 16 January 2023

Academic Editor: Zhaojie Song

Methane (CH_4) microseepage from petroleum basins is a significant contributor to the atmospheric CH_4 budget. However, research about CH_4 migration and release mechanism is still very limited. This work seeks to theorize and verify the migration and release mechanism of CH_4 microseepage via field measurement and physical simulation, which, to the best of our knowledge, has not been reported in literature. Fluxes of CH_4 microseepage from Dawanqi oilfield were measured, and three manifestations of release were observed, namely, continuous, flat, and episodic. Based on field observations, bench-scale physical simulation of CH_4 migration through geological features of the oilfield was further conducted for 290 days. The results show that CH_4 migration is mainly driven by buoyancy and diffusion. In continuous release, CH_4 migration is mainly driven by buoyancy. In flat release, CH_4 migration is dominated by diffusion. At low pressure, CH_4 migrates upward slowly. As buoyancy increases, CH_4 eventually break through the capillary pressure of the pore throat, causing spikes in CH_4 concentrations in the layers above and reproducing episodic release observed during field measurement. Via field observation and verification by physical simulation, this work theorizes the migration mechanism of CH_4 microseepage and its correlation with release types observed and confirms that counterbalance of buoyancy force and capillary pressure plays a critical role in episodic release of CH_4 from oilfield. The findings of this study shed light on the migration mechanism and release manifestations of CH_4 microseepage under different geological conditions and improve accuracy of estimating the flux of CH_4 microseepage into atmosphere.

1. Introduction

Microseepage, the slow and diffuse migration of gaseous hydrocarbons from underground petroleum reservoirs, is an important process that influences gas-oil exploration and the atmospheric methane (CH_4) budget [1, 2].

Since the 1930s, geologists and geochemists have extensively exploited the presence of CH_4 and light alkanes in soil for oil and gas exploration [3–5]. For example, breakthroughs were made in oil and gas exploration in China in the 1950s, with the observation of oil or gas seepage above reservoirs, such as the Karamay oilfield [6]. Since the 1980s, microseepage has been measured and modeled in several petroleum basins of North America and Europe [7–9]. Klusman et al. suggested that knowing the gas flux was also valuable for petroleum exploration and applied the closed chamber method for gas flux measurements in petroleum geology [10]. Several studies found that drylands are not necessarily a net sink for atmospheric CH_4. A substantial portion of drylands occur over sedimentary basins that host natural gas and oil reservoirs, where gas migration to the surface takes place, producing positive fluxes of CH_4 into the atmosphere [11, 12]. Accordingly, research includes microseepage, together with other geological CH_4 exhalation processes (mud volcanoes, oil-gas seeps, and

submarine seepage), in the atmospheric budget of natural CH_4 sources [13–15].

Numerous studies have confirmed that microseepage of CH_4 on the surface (soil, subsoil, and shallow aquifers) originates from deep gas-oil reservoirs [16–18]. There has been a preliminary understanding of CH_4 emissions from shale gas extraction [19–22], production/abandoned oil and gas wells, and their effects on the environment in recent years [23–25]. However, little research focused on the migration and release mechanisms of hydrocarbons [26, 27]. Most researchers have agreed that hydrocarbons that originate from oil reservoirs migrate upward to the surface by buoyancy, advection, and water dissolution [26–29]. Compared with other researchers, we observed three different release manifestations, namely, continuous, flat, and episodic release, on the surface in field work. And on the basis of field results, we discussed the migration mechanism of CH_4 microseepage corresponding to the different release manifestations and potential impact of various geological conditions.

Here, we present the steps of the work (Figure 1). First, Dawanqi oilfield was selected, which has a shallow reservoir. Then, field flux data was measured in Dawanqi oilfield [18]. Next, we built an analog experimental system to study migration mechanism of CH_4 microseepage according to concept model. Finally, CH_4 microseepage release manifestations and migration mechanism were discussed by analyzing the results of field work and physical simulations.

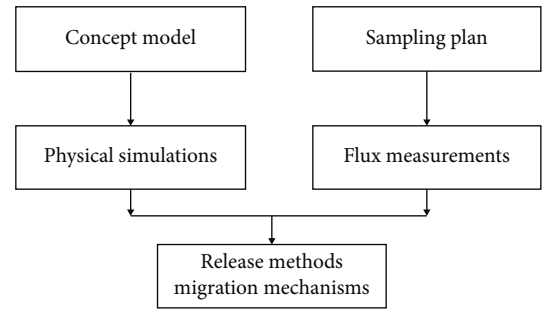

Figure 1: The steps of the work.

2. Geologic Setting

Dawanqi oilfield, located in the western part of the Kuqa-Baicheng depression (Tarim Basin), formed during the terminal stage of the Himalayan movement. The top-down strata of the Dawanqi oilfield (Figure 2(c)) are Quaternary (Q), Neogene Kangcun Formation ($N_{1\text{-}2}k$), Jidike Formation (N_1j), Paleogene Suweiyi Formation, Jurassic, and Triassic coal bearing [6] (see Supplementary Material (available here) for all abbreviations). Hydrocarbon reservoirs are relatively shallow (170–700 m) in the Quaternary to Neogene sandstones; oil and gas were generated in the Triassic and Jurassic coal-bearing formations [30, 31]. The thickness of oil bearing strata reaches 528.9 m, and the depth of groundwater table is 4.2 m [18, 32]. The area has highly faulted and fractured conditions. Three groups of fractures in the northeast (NE), northwest (NW), and eastwest (EW) directions cut the strata into blocks. Geochemical anomalies can be detected when oil and gas that is enriched in block reservoirs migrate to the surface along faults. Gas reservoirs have at least 89 vol% of thermogenic CH_4 ($\delta^{13}C$: −18‰ to −38‰ Vienna Pee Dee Belemnite (VPDB)), with C_{2+} alkanes (8 vol%), N_2 (2 vol%), and CO_2 (0.5 vol%) [33]. During the fieldwork of this study, groundwater can be encountered 4.2 meters below surface.

3. Field Work and Physical Simulations

3.1. Flux Measurements. Field work took place in summer 2014 and 2019 and winter 2015 in the Dawanqi oilfield. The region is characterized by rare vegetarian, low land productivity, and severe climate. The annual temperature ranged from -20°C in winter to 30°C in summer [18]. Figure 2(d) shows that there are 124 flux measurement points across three MT1, MT2, and MT3 [16, 18].

Microseepage CH_4 fluxes were performed with a portable laser-based gas analyzer (UGGA, LGR915-0011, USA; detection limit of 5 ppbv CH_4 and 1σ precision of 0.6 ppbv) combined with a closed accumulation chamber (net volume of 3×10^4 cm^3 and effective height of 7 cm). Each flux measurement was based on accumulation times of ca. 20 min. The sampling interval along each transect varied from 50 to 300 m, depending on suitable ground conditions for installing the closed chamber. The control site was in an area located outside the petroleum field, 50 km from the field boundary.

3.2. Analog Experimental System. To study migration mechanism of CH_4 microseepage, physical simulations were conducted in an intermedia-scale apparatus, which had internal dimensions of $100 \times 100 \times 120$ cm^3. Since migration of CH_4 microseepage corresponds to many factors, such as dynamic systems, channel conditions, and geochemical shielding, it was not possible to consider all geological aspects within one apparatus. The main controlling factors (gas source, caprock, and migration channel) were chosen to establish a concept model (Figure 2(a)). In terms of migration channels, microfissures in strata were considered, and complex factors such as faults, unconformities, and strata tilt were excluded.

The cell was fitted with sampling ports at 20 cm intervals along the height of the cell. Layers 1–5 were packed with cement and quartz sand. In Figure 3(b), layer 1 and layers 2–5 represent the simulated caprock and overlying strata, respectively. The porosity, permeability, and breakthrough pressure of simulated caprock were 16.48%, 0.095 mD, and 1.56 MPa, respectively, equivalent to caprock V [34]. The height of saturation zone was about to 15 cm at layer 1. This layer provided a wet-sealing system which avoids gas emitted. In the top, 25 cm soil (layers 6 and 7) was supported by a stainless-steel frame.

A point source injection was used to replicate buoyancy-driven vertical migration, placed 6.5 cm from the bottom boundary (Figure 4). Natural gas was supplied from a cylinder, with batch composition of CH_4 (89%), C_{2+} (4.4%), C_{3+} (2.3%), C_{4+} (1.7%), C_{4+} (0.2%), and N_2 (2.4%), in accordance with a wet gas reservoir of the Kuqa oil-gas system. Gas pressure was measured at the injection point of cylinder and apparatus

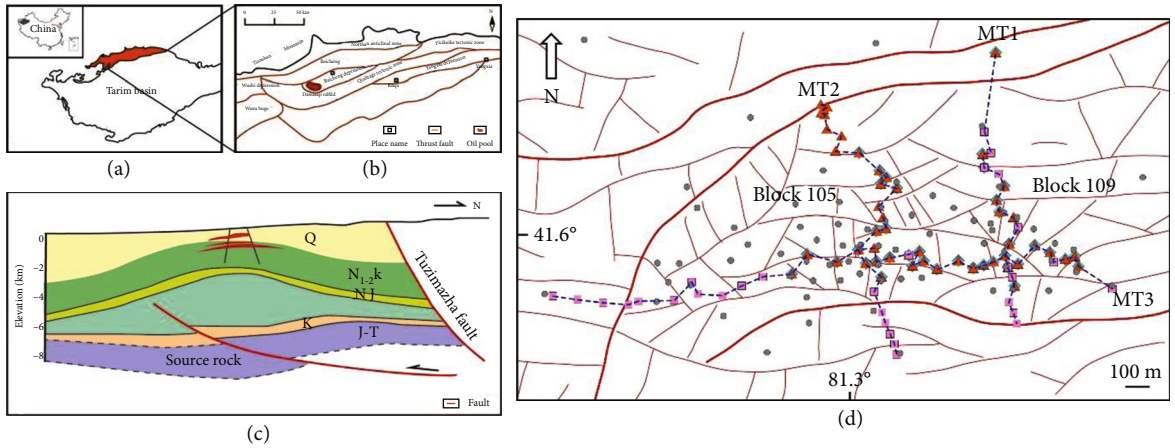

FIGURE 2: (a) Location of Tarim Basin. (b) Location and strata structure of Dawanqi oilfield. (c) Diagram of Dawanqi oilfield section. (d) Gas flux measurement locations at the Dawanqi oilfield. Red lines are fault and fracture systems identified by geophysical prospections [18]. Gray circles are oil wells. Triangles (August 2014), diamonds (January 2015), and squares (August 2019) are the measurement sites of each measurement campaign.

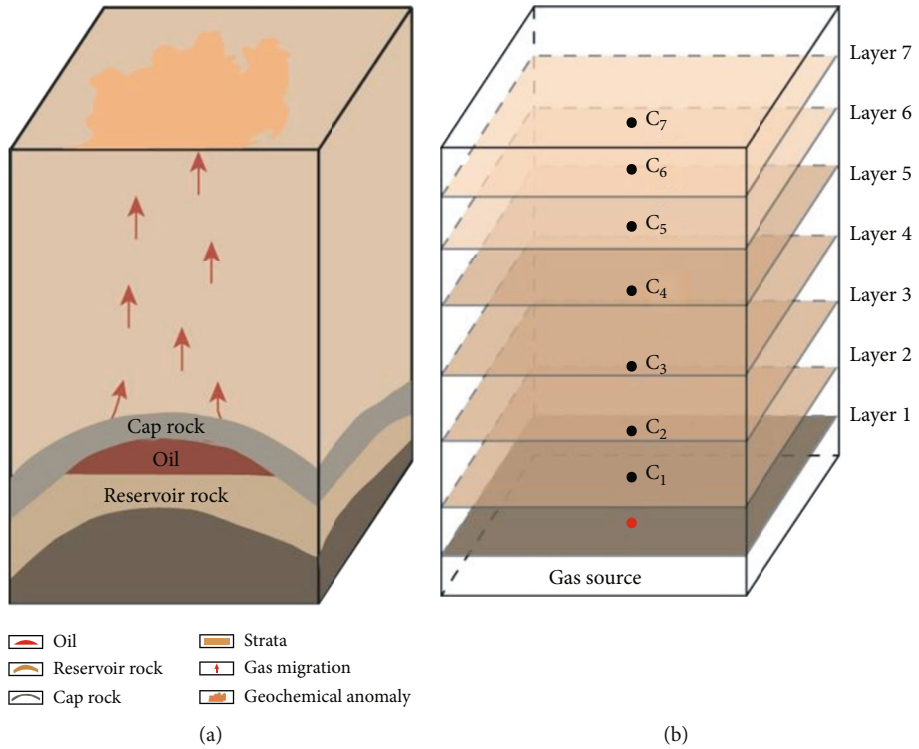

FIGURE 3: (a) Microseepage CH_4 vertical migration concept model. (b) Sketch of delineation of layers.

using a gas pressure meter connected to the gas injection tube, providing a constant gas flow during injection.

Based on the pressure program, the entire injection process was divided into three phases, namely, phase 1 (days 1-78), phase 2 (days 79-119), and phase 3 (days 120-290). The total gas pressure of Phase 1 and Phase 2 is 0.02MPa and 0.1MPa, respectively. Finally, phase 3 was initiated on day 120 with a total gas pressure of 0.2 MPa.

The sampling tube fitted on one end with sampling probe and the other end of the tube extending outside. 50 μL gas samples were extracted from the sampling tube for composition analyses. The CH_4 concentrations in the gas samples were analyzed with an Agilent 6890 N gas chromatograph equipped with a flame ionization detector. The concentrations of CH_4 were determined with a precision of 0.01 ppm.

4. Results

4.1. Release Types of CH_4 Microseepage. During field measurements, release of CH_4 microseepage can be categorized as three types, namely, continuous (Figure 5), flat (Figure 6),

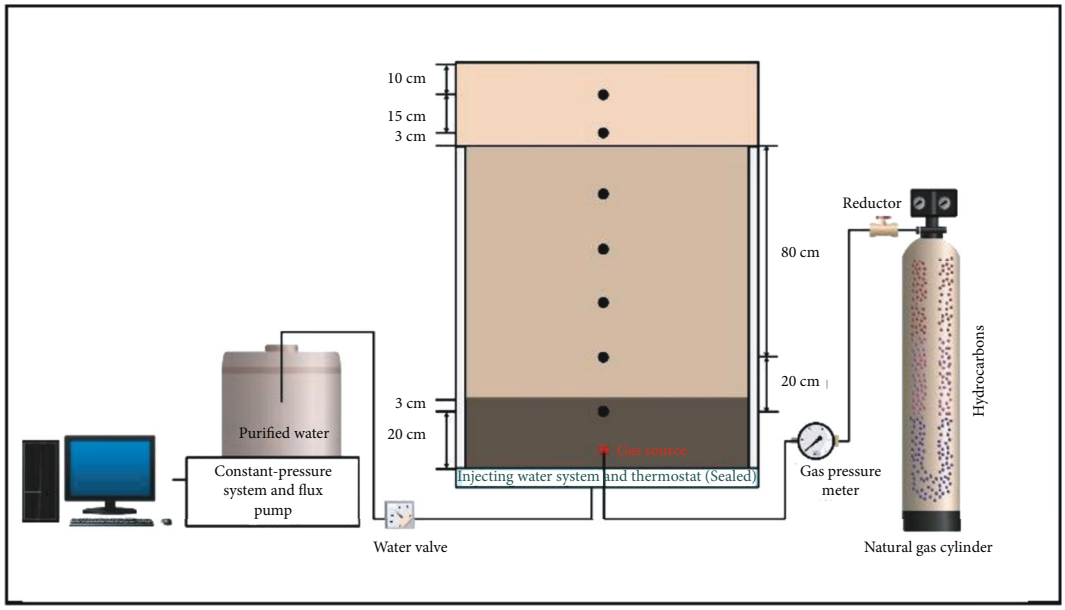

Figure 4: Sketch of the experimental apparatus.

and episodic release (Figure 7). As shown in Table 1, continuous release mainly occurs near faults, with CH_4 fluxes substantially higher than other release types. In continuous release, CH_4 concentration elevates quickly and stably, at the rate of 0.007 ppm/second at 545-12 and by 0.285 ppm/second at 555-16 (Figure 5). In contrast, flat release refers to the case where CH_4 concentration changes at nugatory rates ($<10^{-4}$ ppm/second; see Figure 6(a)).

Episodic release is defined as spikes of CH_4 concentration measurement (Figure 7), which occurs along faults or oil-gas area. Episodic release can be further divided into two types, i.e., the spike and the flat type. The spike type, shown in Figures 7(a) and 7(c), features spikes of CH_4 concentration followed by rapid decline. The flat type, on the other hand, presents high CH_4 concentration plateaued for more than 100 seconds, due to consistently high pressure (Figures 7(b) and 7(d)). Moreover, Figure 7 indicates that the interval for episodic release is ca. 2000 seconds, demonstrating that the episodic release is a stochastic event primarily due to the counterbalance between buoyancy and capillary pressure (see Section 5.1).

4.2. Physical Simulations of CH_4 Microseepage. The initial pressure was set to 0.02 MPa for phase 1 of the physical simulation conducted (days 1–78), as the breakthrough pressure for microseepage was relatively low. The pressure was then increased to 0.1 MPa for phase 2 (days 79–119) and 0.2 MPa for phase 3 (days 120-190).

4.2.1. CH_4 Concentration in Simulated Caprock and Strata. As shown in Table 2 and Figure 8(a), CH_4 concentration gradually decreases from layer 1 to layer 3. As shown in Figures 8(b)–8(d), CH_4 concentrations at all these layers remain relatively stable during phases 1 and 2 but rapidly increase from days 140 to 150 during phase 3, resulting high standard deviation (SD) variations. At layer 1, the SD substantially increases to 5827.44, accompanied by apparent episodic release. Note that the episodic release (days 142–145) was delayed from pressure increase at the start of phase 3 (day 120). This delay indicates that pressure increase does not directly lead to episodic release. Only after the buoyancy increases and breaks through the capillary pressure can episodic release occur.

4.2.2. CH_4 Concentration in Soil. Figures 8(e) and 8(f) show that CH_4 concentrations (8.55–1919.26 ppm) at layer 7 are higher than those at layer 6 (6.45–800 ppm). Several spikes can be seen on both layers, which are similar to the episodic release observed in the field measurements at 543-28-5 (see Figure 7(c)). The presence of microfissure or fault in simulated caprock or strata, as confirmed by scanning electron microscopic (SEM) imaging (see Figure 9), suggests that priority paths may exist and thus cause the spikes observed on layers 6 and 7. This mechanism differs from that for layers 1-3 at days 142-150 (namely, buoyancy; see Section 4.2.1). These findings also imply that failure to observe and record episodic release events may substantially underestimate CH_4 fluxes.

5. Discussions

5.1. Release Mechanism of CH_4 Microseepage in Field Work. Continuous release (Figure 5) is mainly distributed along faults, which form preferential pathway for the upward migration of CH_4 microbubbles. CH_4 migration along these channels is evidenced by several studies [35–37]. Preferential pathway, which has the minimum resistance and maximum buoyancy, determines the direction of CH_4 migration [38]. In addition, fault sealability can influence the migration and release mechanism of CH_4 microseepage. Unoxidized CH_4 can be released into the atmosphere and manifest as continuous release when faults extend to the Earth's surface [39].

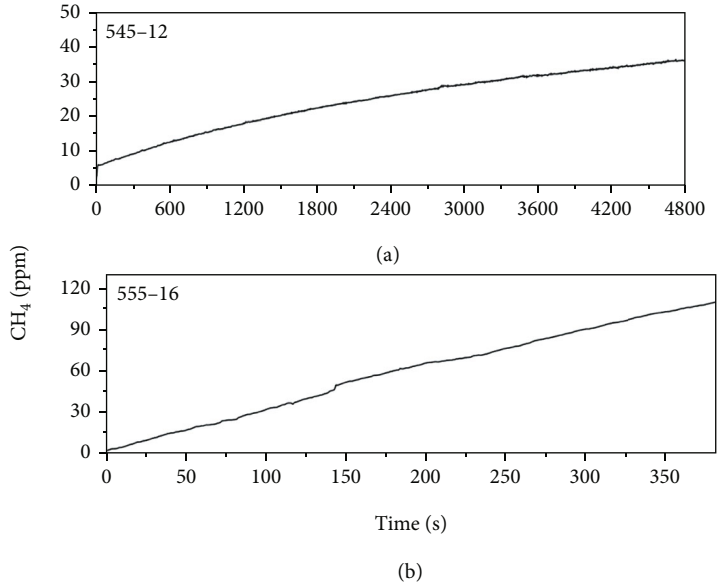

Figure 5: Continuous release: (a) 545-12; (b) 555-16.

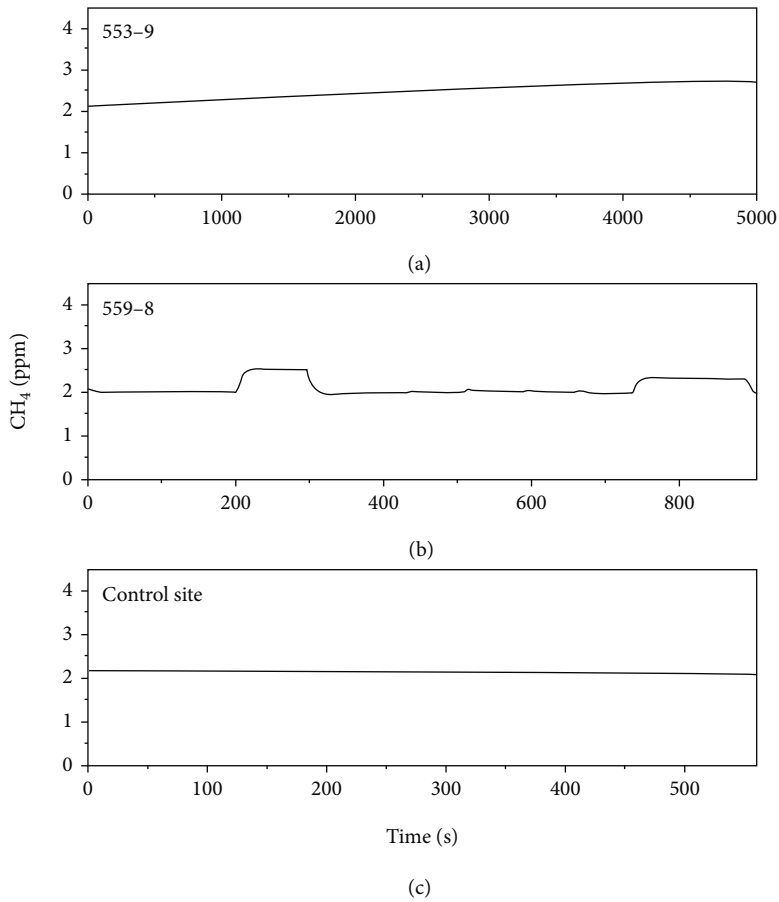

Figure 6: Flat release: (a) 553-9; (b) 559-8; (c) control site.

Robertson et al. advocate that diffusion or buoyancy may cause continuous or discontinuous gas migration [40]. Flat release shown in Figures 6(a) and 6(b) implies substantially lower CH_4 migration rate than continuous release driven by buoyancy. Therefore, flat release is likely to be driven by diffusion, which is caused by concentration gradient, regardless of dynamic systems, porosity, permeability, or capillary pressure. In addition, diffusion plays essential role in oil

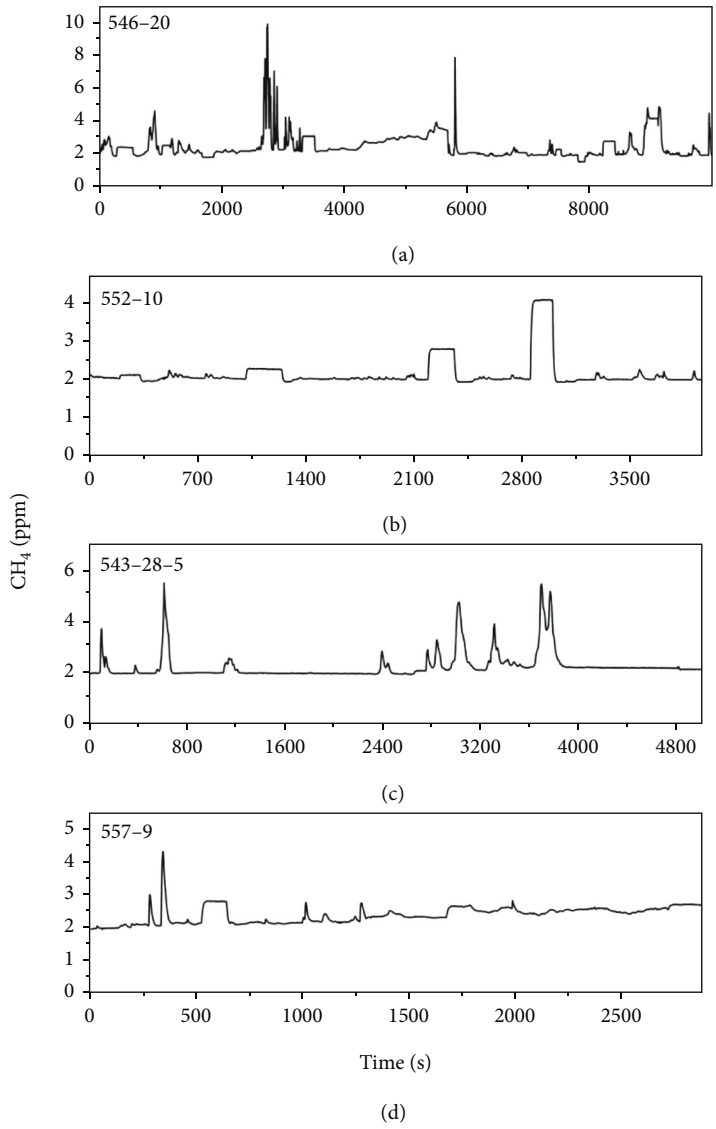

Figure 7: Episodic release: (a) 546-20; (b) 552-10; (c) 543-28-5; (d) 557-9.

Table 1: CH_4 microseepage fluxes and release types of some sampling points in the Dawanqi oilfield.

Site	Flux ($mg \cdot m^{-2} \cdot d^{-1}$)	Release types	Location
545-12	69.2	Continuous release	Fault
555-16	329.9		Fault
546-20	1.58	Episodic release	Fault
552-10	1.12		Oil-gas area
543-28-5	0.1		Fault
557-9	1.14		Oil-gas area
553-9	12.53	Flat release	Oil-gas area
559-8	0.76		Fault
Control site	0.24	—	—

Table 2: Statistics of CH_4 concentration (layers 1–3).

Group	Day (d^{-1})	Max (ppm)	Min (ppm)	Std. dev
Layer 1	1–78	1864.84	278.49	316.11
	79–119	2128.08	1325.48	180.95
	120–290	31502.13	1782.43	5827.44
Layer 2	1–78	712.93	80.07	96.46
	79–119	319.81	142.27	37.27
	120–290	5299.93	85.42	1574.67
Layer 3	1–78	428.21	39.75	74.38
	79–119	133.75	54.71	16.30
	120–290	902.53	49.29	252.80

and gas loss of shallow reservoirs. It is estimated that Dawanqi oilfield, which is geographically characterized with shallow hydrocarbon reservoirs, highly distributed fault systems, and poor cover conditions, lost 5.5%, 25.6%, and 77.9% of the reserves in the Quaternary (2.0 Ma), Pliocene (5.2 Ma), and Miocene (23.2 Ma), respectively, mainly due to diffusion [32]. However, some other researchers suggest

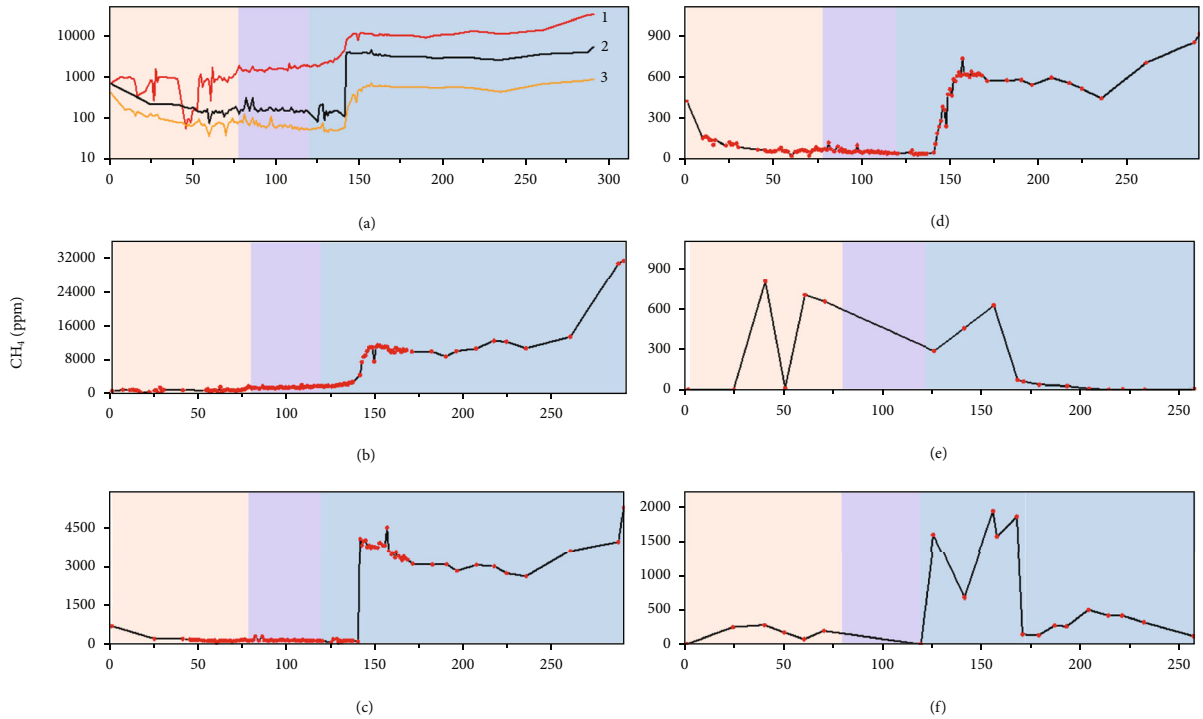

Figure 8: CH_4 concentration in different central points: (a) layers 1-3; (b) layer 1; (c) layer 2; (d) layer 3; (e) layer 6; (f) layer 7.

that diffusion is not the main reason for gas migration [1, 41]. After all, reservoirs would not have formed or preserved if oil and gas could diffuse through the overlying strata and easily escape to the surface. Nonetheless, diffusion should not be ignored especially when CH_4 migrates to a well-sealed area (such as mudstone). If there were no faults or microfissures in the overlying strata, CH_4 can diffuse upward slowly and exhibit flat release on the surface. The release rate is higher than that in the control site (Figure 7(c)) but lower than in episodic and continuous release area.

Episodic release (Figure 7) occurs both along faults and oil-gas areas. Heterogeneous environments can cause lateral or pulsed gas transport in porous media [42–44]. As CH_4 trapped under caprock gradually accumulates, its buoyant force increases. Eventually, buoyancy overcomes the capillary pressure, so that CH_4 breaks through the pore throat in caprock [45–47], migrates upward, and causes microseepage [48, 49]. After that, the buoyancy decreases below the threshold, and hydrocarbons start to accumulate again. Another example of this process is the Old Faithful geyser in Yellowstone National Park in Wyoming, USA. In addition, episodic release is also caused by discontinuous gas flow. As shown in the scheme of flux measurement (Figure 10), CH_4 floats to the top of the closed chamber (blue area) owing to low density. If the gas in the entire chamber had not thoroughly mixed, the top part rich in CH_4 would be sampled, hence a concentration spike in the measurement. Subsequently, due to diffusion driven by concentration gradient, CH_4 concentration measurement started to decrease and eventually returned to average concentration of CH_4 accumulated in the chamber, which was still higher than the initial value measured at the beginning of sampling process. Barometric pressure and wind intensity may also influence CH_4 release types on the surface [50–52]. In the Tarim Basin where this study was conducted, the variation of the barometric pressure was relatively small; however, the velocity (0.3-5 m/s) and direction of the wind changed rapidly based on field measurements, whose impact on CH_4 release manifestations observed remains to be clarified.

5.2. Migration Mechanism of CH_4 Microseepage in Physical Simulations. In our previous study, Wang et al. have demonstrated that vertical migration of CH_4 microseepage is driven by buoyancy at layers 1–3 and by diffusion at layers 4 and 5 in physical simulation [33]. Combined with field measurement, we therefore advocate that either buoyancy or diffusion will be the dominant driving force under different circumstances. Specifically, CH_4 microseepage is mainly driven by buoyancy in intense tectonic deformation, highly fracture/microfracture zone, and poorly sealed channels; when CH_4 migrates to highly sealed caprock or vadose zone, diffusion becomes the leading migration mechanism.

Admittedly, the bench-scale apparatus used in this work is much lower in pressure and smaller in scale than the actual oil reservoir, in addition to many other geological features that cannot be reproduced perfectly. Nonetheless, the physical simulation results of this work theorize the influence of buoyancy force, capillary pressure, and preferential pathway on release types of CH_4 microseepage.

6. Summary and Conclusions

The main conclusion remarks of this study can be summarized as follows:

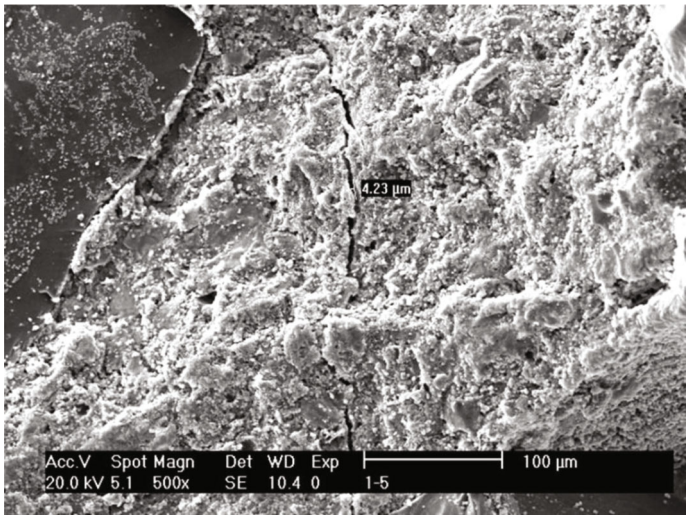

Figure 9: SEM imaging of simulated caprock.

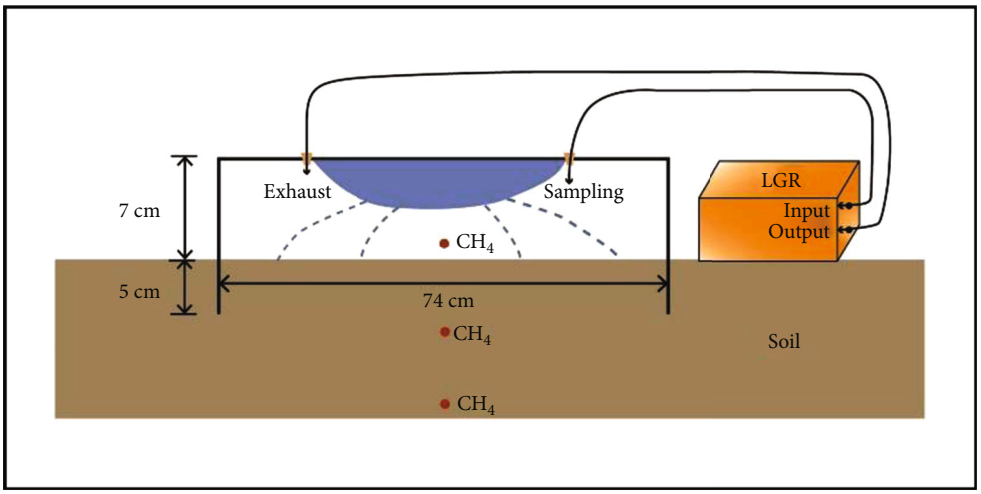

Figure 10: Scheme of CH_4 microseepage flux measurements.

(i) Three CH_4 microseepage release manifestations were observed in field measurement: (1) continuous, (2) flat, and (3) episodic

(ii) The results of physical simulations illustrate that these CH_4 release manifestations can be attributed to various factors of CH_4 migration, such as preferential pathway, buoyancy force, and capillary pressure

(iii) It is theorized that in each CH_4 release manifestation, its migration is subjected to different geological conditions and dominated by one specific mechanism of buoyancy or diffusion and thus differs from one another

(iv) In continuous release, CH_4 migrates along preferential pathway (microfissure or fault) at high speed and concentration, mainly driven by buoyancy. In flat release, CH_4 migration is dominated by diffusion, causing its concentration to increase at a rate lower than continuous release but higher than control. In episodic release, CH_4 travels along microfissures driven by buoyancy at highly fluctuating concentration

(v) CH_4 fluxes might be underestimated if it fails to record episodic release events

Surveys on geological CH_4 fluxes over the past 20 years have confirmed their significant contribution to atmospheric CH_4, but more thorough investigation on CH_4 microseepage mechanisms, emission monitoring, and prediction models will be essential to improving the accuracy of quantifying greenhouse gas emissions in the future. The CH_4 microseepage release manifestations and corresponding CH_4 migration mechanism discussed in this paper are based on field monitoring data and physical simulations, which may differ from the actual geological environment. After all, the migration mechanism changes with the change of the geological conditions.

Data Availability

The data used to support the findings of this study are included within the article.

Disclosure

Part of the research was carried out at the Wuxi Research Institute of Petroleum Geology, Research Institute of Petroleum Exploration and Production, SINOPEC, Wuxi, China.

Conflicts of Interest

The authors declare that there are no conflicts of interest regarding the publication of this paper.

Acknowledgments

This work was supported by the Joint Funds of the National Natural Science Foundation of China (grants U2003101 and 41872126) and the Graduate Scientific Research Foundation of Hangzhou Dianzi University (CXJJ2021030 and 2022R407B059).

Supplementary Materials

All abbreviations within the article and their corresponding full names are listed in the table. *(Supplementary Materials)*

References

[1] G. Ciotoli, M. Procesi, G. Etiope, U. Fracassi, and G. Ventura, "Influence of tectonics on global scale distribution of geological methane emissions," *Nature Communications*, vol. 11, no. 1, pp. 1–8, 2020.

[2] A. Mazzini, A. Sciarra, G. Etiope et al., "Relevant methane emission to the atmosphere from a geological gas manifestation," *Scientific Reports*, vol. 11, no. 1, p. 4138, 2021.

[3] G. Laubmeyer, "A new geophysical prospecting method, especially for deposits of hydrocarbons," *Petroleum*, vol. 29, pp. 1–4, 1933.

[4] V. T. Jones and R. J. Drozd, "Predictions of oil or gas potential by near-surface geochemistry," *AAPG Bulletin*, vol. 67, no. 6, pp. 932–952, 1983.

[5] D. Schumacher and M. A. Abrams, *Hydrocarbon Migration and Its Near-Surface Expression*, Tulsa: American Association of Petroleum Geologist, 1996.

[6] Y. C. Chen, Z. M. Shen, and Y. J. Li, "Simulation of diffusion quantity of solution gas in Dawanqi oil field," *Petroleum Exploration and Development*, vol. 29, pp. 58–60, 2002.

[7] R. W. Klusman, *Soil Gas and Related Methods for Natural Resource Exploration*, John Wiley & Sons Inc., New York, 1994.

[8] D. Schumacher and L. A. LeSchack, *Surface Exploration Case Histories: Applications of Geoschemistry, Magnetics, and Remote Sensing*, American Association of Petroleum Geologists, 2002.

[9] H. Sechman, "Detailed compositional analysis of hydrocarbons in soil gases above multi-horizon petroleum deposits - a case study from western Poland," *Applied Geochemistry*, vol. 27, no. 10, pp. 2130–2147, 2012.

[10] R. W. Klusman, M. E. Leopold, and M. P. LeRoy, "Seasonal variation in methane fluxes from sedimentary basins to the atmosphere: results from chamber measurements and modeling of transport from deep sources," *Journal of Geophysical Research: Atmospheres*, vol. 105, no. D20, pp. 24661–24670, 2000.

[11] R. W. Klusman, M. E. Jakel, and M. P. LeRoy, "Does microseepage of methane and light hydrocarbons contribute to the atmospheric budget of methane and to global climate change?," *Association of Petroleum Geochemical Explorationists Bulletin*, vol. 11, pp. 1–55, 1998.

[12] G. Etiope and R. W. Klusman, "Microseepage in drylands: flux and implications in the global atmospheric source/sink budget of methane," *Global and Planetary Change*, vol. 72, no. 4, pp. 265–274, 2010.

[13] G. Etiope, G. Ciotoli, S. Schwietzke, and M. Schoell, "Gridded maps of geological methane emissions and their isotopic signature," *Earth System Science Data*, vol. 11, no. 1, pp. 1–22, 2019.

[14] G. Etiope and S. Schwietzke, "Global geological methane emissions: an update of top-down and bottom-up estimates," *Elementa: Science of the Anthropocen*, vol. 7, pp. 1–9, 2019.

[15] M. Saunois, A. R. Stavert, B. Poulter et al., "The global methane budget 2000–2017," *Earth System Science Data*, vol. 12, no. 3, pp. 1561–1623, 2020.

[16] J. H. Tang, Y. Xu, G. Wang et al., "Microseepage of methane to the atmosphere from the Dawanqi oil-gas field, Tarim Basin, China," *Journal of Geophysical Research-Atmospheres*, vol. 122, no. 8, pp. 4353–4363, 2017.

[17] J. H. Tang, Y. Xu, G. Wang et al., "Methane in soil gas and its migration to the atmosphere in the Dawanqi oilfield, Tarim Basin, China," *Geofluids*, vol. 2019, Article ID 1693746, 10 pages, 2019.

[18] Y. Zhao, G. Wang, G. Etiope et al., "Seasonal variation of methane microseepage in the Dawanqi oilfield (China): a possible climatic control," *Journal of Geophysical Research: Atmospheres*, vol. 126, no. 10, 2021.

[19] D. L. Pinti, Y. Gelinas, A. M. Moritz, M. Larocque, and Y. Sano, "Anthropogenic and natural methane emissions from a shale gas exploration area of Quebec, Canada," *Science of the Total Environment*, vol. 566–567, pp. 1329–1338, 2016.

[20] M. Annevelink, J. A. J. Meesters, and A. J. Hendriks, "Environmental contamination due to shale gas development," *Science of the Total Environment*, vol. 550, pp. 431–438, 2016.

[21] A. Schimmelmann, S. A. Ensminger, A. Drobniak et al., "Natural geological seepage of hydrocarbon gas in the Appalachian Basin and Midwest USA in relation to shale tectonic fracturing and past industrial hydrocarbon production," *Science of the Total Environment*, vol. 644, pp. 982–993, 2018.

[22] D. Lowry, R. E. Fisher, J. L. France et al., "Environmental baseline monitoring for shale gas development in the UK: identification and geochemical characterisation of local source emissions of methane to atmosphere," *Science of the Total Environment*, vol. 708, article 134600, 2020.

[23] I. M. Boothroyd, S. Almond, S. M. Qassim, F. Worrall, and R. J. Davies, "Fugitive emissions of methane from abandoned, decommissioned oil and gas wells," *Science of the Total Environment*, vol. 547, pp. 461–469, 2016.

[24] O. N. Forde, K. U. Mayer, and D. Hunkeler, "Identification, spatial extent and distribution of fugitive gas migration on

the well pad scale," *Science of the Total Environment*, vol. 652, pp. 356–366, 2019.

[25] G. Schout, J. Griffioen, S. M. Hassanizadeh, G. Cardon de Lichtbuer, and N. Hartog, "Occurrence and fate of methane leakage from cut and buried abandoned gas wells in the Netherlands," *Science of the Total Environment*, vol. 659, pp. 773–782, 2019.

[26] R. W. Klusman and M. A. Saeed, *Comparison of Light Hydrocarbon Microseepage Mechanisms*, The American Association of Petroleum Geologists, 1996.

[27] A. Brown, "Evaluation of possible gas microseepage mechanisms," *AAPG Bulletin*, vol. 84, no. 11, pp. 1775–1789, 2000.

[28] R. MacElavain, "Mechanics of gaseous ascension through a sedimentary column," in *Unconventional Methods in Exploration for Petroleum and Natural Gas*, pp. 15–28, Southern Methodist University, Dallas, 1969.

[29] L. C. Price, "A critical overview and proposed working model of surface geochemical exploration min unconventional method IV," in *Unconventional Methods in Exploration for Petroleum and Natural Gas IV*, pp. 245–304, Southern Methodist University Press, Dallas, 1986.

[30] H. Kuang, S. Niu, and X. Chen, "The diagenetic characteristics and its controlling factors of the Kangcun formation in the Dawanqi oilfield, the Tarim Basin (in Chinese)," *Geoscience*, vol. 17, no. 2, pp. 211–216, 2003.

[31] H. Kuang and G. Jin, "Reservoir characteristic and evalution of the Kangcun formation in the Dawanqi oilfield Tarim Basin," *Journal of Geomechanics*, vol. 11, no. 1, pp. 81–89, 2005.

[32] M. Zhao, Y. Song, S. Liu, and S. Jiang, "The diffusion influence on gas pool: Dawanqi oilfield as an example," *Natural Gas Geoscience*, vol. 14, no. 5, pp. 393–397, 2003.

[33] G. Wang, Y. Tang, T. Cheng, J. Tang, M. Fan, and L. Lu, "Laboratory simulation of the formation process of surface geochemical anomalies applied to hydrocarbon exploration," *Acta Geologica Sinica-English Edition*, vol. 90, no. 6, pp. 2149–2162, 2016.

[34] X. You, "Study on assessment method of caprocks in natural gas pools," *Oil & Gas Geology*, vol. 12, no. 3, pp. 261–275, 1991.

[35] G. Etiope and S. Lombardi, "Evidence for radon transport by carrier gas through faulted clays in Italy," *Journal of Radioanalytical and Nuclear Chemistry, Articles*, vol. 193, no. 2, pp. 291–300, 1995.

[36] G. Etiope, "Subsoil CO2 and CH4 and their advective transfer from faulted grassland to the atmosphere," *Journal of Geophysical Research: Atmospheres*, vol. 104, no. D14, pp. 16889–16894, 1999.

[37] N. Voltattorni, D. Cinti, L. Pizzino, and A. Sciarra, "Statistical approach for the geochemical signature of two active normal faults in the western Corinth gulf rift (Greece)," *Applied Geochemistry*, vol. 51, pp. 86–100, 2014.

[38] Z. Jiang, X. Pang, J. Zeng, H. Wang, and Q. Luo, "Research on types of the dominant migration pathway sand their physical simulation experiment (in Chinese)," *Earth Science Frontier*, vol. 12, no. 4, pp. 507–516, 2005.

[39] O. N. Forde, K. U. Mayer, A. G. Cahill, B. Mayer, J. A. Cherry, and B. L. Parker, "Vadose zone gas migration and surface effluxes after a controlled natural gas release into an unconfined shallow aquifer," *Vadose Zone Journal*, vol. 17, no. 1, article 180033, 2018.

[40] J. O. Robertson, G. Chilingar, L. Khilyuk, and B. Endres, "Migration of gas from oil/gas fields," *Energy Sources, Part A: Recovery, Utilization, and Environmental Effects*, vol. 34, no. 15, pp. 1436–1447, 2012.

[41] G. Etiope, "Natural gas seepage," in *The Earth's Hydrocarbon Degassing*, Springer, Switzerland, 2015.

[42] D. W. Tomlinson, N. R. Thomson, R. L. Johnson, and J. D. Redman, "Air distribution in the Borden aquifer during in situ air sparging," *Journal of Contaminant Hydrology*, vol. 67, no. 1-4, pp. 113–132, 2003.

[43] K. G. Mumford, J. E. Smith, and S. E. Dickson, "The effect of spontaneous gas expansion and mobilization on the aqueous-phase concentrations above a dense non-aqueous phase liquid pool," *Advances in Water Resources*, vol. 33, no. 4, pp. 504–513, 2010.

[44] C. M. Steelman, D. R. Klazinga, A. G. Cahill, A. L. Endres, and B. L. Parker, "Monitoring the evolution and migration of a methane gas plume in an unconfined sandy aquifer using time-lapse GPR and ERT," *Journal of Contaminant Hydrology*, vol. 205, pp. 12–24, 2017.

[45] P. Bretan, G. Yielding, and H. Jones, "Using calibrated shale gouge ratio to estimate hydrocarbon column heights," *AAPG Bulletin*, vol. 87, no. 3, pp. 397–413, 2003.

[46] A. W. Gorody, "Factors affecting the variability of stray gas concentration and composition in groundwater," *Environmental Geosciences*, vol. 19, no. 1, pp. 17–31, 2012.

[47] C. Ma, C. Lin, C. Dong et al., "Quantitative relationship between argillaceous caprock thickness and maximum sealed hydrocarbon column height," *Natural Resources Research*, vol. 29, no. 3, pp. 2033–2049, 2020.

[48] S. Hao, Z. Huang, and J. Yang, *Dynamic Balance of Natural Gas Migration and Accumulation and Its Application*, Petroleum Industry Press, Beijing, 1994.

[49] S. Hao, Y. Gao, and Z. Huang, "Characteristics of dynamic equilibrium for natural gas migration and accumulation of the gas field in the center of the Ordos Basin," *Science in China Series D: Earth Sciences*, vol. 40, no. 1, pp. 11–15, 1997.

[50] R. H. Nilson, E. W. Peterson, K. H. Lie, N. R. Burkhard, and J. R. Hearst, "Atmospheric pumping: a mechanism causing vertical transport of contaminated gases through fractured permeable media," *Journal of Geophysical Research: Solid Earth*, vol. 96, no. B13, pp. 21933–21948, 1991.

[51] J. Massmann and D. F. Farrier, "Effects of atmospheric pressures on gas transport in the vadose zone," *Water Resources Research*, vol. 28, no. 3, pp. 777–791, 1992.

[52] G. Etiope and D. Z. Oehler, "Methane spikes, background seasonality and non-detections on Mars: a geological perspective," *Planetary and Space Science*, vol. 168, pp. 52–61, 2019.